The hierarchical organization in biomaterials: from nanoparticles via mesocrystals to functionality

/ Wolfgang W. Schmahl *(1)* / Klemens Kelm *(2)* / Erika Griesshaber *(1)* / Andreas Goetz *(1)* / Guntram Jordan *(1)* / Dayin Xu *(1)* / Casjen Merkel *(1)* / Uwe Brand *(3)* / Alan Logan *(4)*

(1) GeoBioCenter^{LMU} and Dept. of Earth and Environmental Sciences, LMU Munich, Germany.
(2) DLR-Institut für Werkstoff-Forschung, Köln-Porz, Germany.
(3) Dept. of Earth Sciences, Brock University, St. Catharines, Ontario, Canada.
(4) Dept. of Physical Sciences, University of New Brunswick, Saint John, New Brunswick, Canada.

Abstract

As opposed to most human made materials, biologic structural materials employed for skeletons or teeth show a hierarchical architecture, where the components of organic macromolecules and mineral substance are inter-weaved on many length scales in order to form a composite material. In the overall skeleton the organic biopolymer fibres provide flexibility and tensile strength while the mineral provides a high elastic modulus, compressive strength, hardness and resistance to abrasion. The hierarchical composite architecture provides fracture toughness. The morphogenesis of the biomaterial as a whole and of the mineral particles is guided by the organic matrix. In this paper we use the example of rhynchonelliform brachiopods to discuss the nano- to macroscale assemblage.

Key-words: Biomineralization, Calcite, Hierarchical Structure, Organic Matrix, Amorphous Calcium Carbonate (ACC), Texture, Hybrid Fibre Composite, Brachiopods

1. Introduction

Biological hard tissues have attracted much attention for several decades since they are both a library of information on the evolution of life and its environmental conditions but they are also a rich source of prototypes for an advanced materials design *(e.g. Currey 1999; Currey 2006; Gao 2006; Fratzl and Weinkammer, 2007)*. Earth scientists have used the isotope and trace element signature of marine shells to reconstruct sea water temperatures *(e.g. Veizer et al., 1999; Buening, 2001; Brandt et al., 2003)*. Initially it was generally believed that the carbonate minerals of shells or corals form in equilibrium with sea water *(Lowenstam, 1961)* such that the results of in-vitro fractionation experiments could potentially be used to deduce water temperatures from isotope ratios and from trace element concentration *(Lowenstam, 1961, Mucci & Morse, 1983, Carpenter & Lohmann, 1992)*. However, it became clear later on, that these chemical signatures are differentiated for different organisms and for different parts of the same specimen *(e.g. Auclair et al., 2003; Carpenter and Lohmann, 1995; Parkinson et al., 2005)*. This implies that biomineralization does not occur in an equilibrium with sea water. This phenomenon is referred to as the vital effect *(Weiner & Dove, 2003)*. Anthropologists and archaeologists use the evidence preserved in the bone mineral for many purposes. In their case the identification of post-mortem changes in the material such as diagenesis is important in the chain of evidence leading to any sound conclusion. Therefore, the knowledge of the original structure and - if possible - any clue towards the processes of biosynthesis and morphogenesis are indispensable for forensic interpretations of hard biomaterials.

Investigations of the mechanical strength of nacre-based shell materials *(Currey & Taylor, 1974,*

Currey, 1977; Jackson, 1988; Barthelat & Espinosa, 2007) lead to the insight that these natural materials are superior to many engineering products when strength and toughness in relation to mass are considered *(Sarikaya & Aksay, 1995)*. By now several models have been proposed why nacre achieves its strength owing to the microstructure of "mineral platelets embedded in a thin organic matrix" *(Okumura & de Gennes, 2001; Katti et al., 2005; Gao, 2006)*.

While nacre and other parts of mollusc shells have been investigated by numerous scientists, we turned our attention to brachiopods, a phylum of sessile marine species, which produce either calcitic (the *Rhynchonelliformea and Craniiformea*) or phosphatic (the *Linguliformea*) shells. Brachiopods have been existing since the Cambrian or even the late Precambrian *(Williams et al., 2000)*. A review focussing mainly on the material architecture of the phosphatic forms has recently been published *(Schmahl et al., 2008)*. Here we focus on the hierarchical architecture of the calcitic forms.

2. Experimental

The examination of a hierarchical structure involves diffraction and microscopy techniques on several length scales. Mineral phases were identified by x ray diffraction on a STOE focussing transmission diffractometer operated with Mo-Kα_1-radiation. High-resolution imaging and diffraction was performed on a Philips CM30T electron microscope equipped with a Noran EDX system and an HPGe detector. Electron energy-loss spectrometry (EELS) analyses were done with a Gatan PEELS 666. Scanning electron micrographs were obtained on a LEO Gemini 1530 SEM and a JEOL JSM-6500 SEM using an accelerating voltage of 5 to 12 kV and a beam current of 3.0 nA. Electron backscatter diffraction (EBSD) was performed with the SEMs by using the HKL EBSD system. It provides crystallographic orientation information from the sub-micrometer- to the sub-millimetre-scale. The JPK NanoWizard® AFM system was used for observation of the nanoparticles. AFM images were taken in dry and wet conditions. Contact and intermittent contact modes were applied. By using different organic and inorganic solutions in the AFM cell organic and inorganic components of the material were dissolved selectively. For dissolving the mineral component we have used distilled water and EDTA solution. Taking the enzymes trypsin (in tris buffer) and chitinase (in McIlvine buffer), we could dissolve the organic biomaterial component.

Organic polymers present within the shells were fixed chemically with glutaraldehyde immediately after removal of the animals from the sea water. The samples were left in the solution for 12 to 24 hours. Subsequently the samples were washed repeatedly with a phosphate buffer and were stored for longer time periods in the buffer. Fresh phosphate buffer is prepared every month and is exchanged monthly.

3. Results and Interpretation

3.1 Overview

Biology constructs its materials from bottom-up and thus a hierarchical structure develops in a natural way in the best sense of the word "natural", and quite opposite to the colloquial meaning of the word "hierarchy". The description of a hierarchical structure can take a top-down or a bottom-up approach; both have their advantages and disadvantages. Following the biologic construction principle we take the bottom-up approach in the discussion below. However, the description will necessarily need to jump between different length scales, therefore a brief overview over the main terms used is given in Table 1. The reader is advised to inspect Table 1 before proceeding to the detailed description. Most importantly, brachiopods produce three distinct main material fabrics with different crystallite morphologies of the calcite: (1) the so-called primary layer material with small, frequently nanoscale, and less regularly shaped crystallites, (2) a fibre composite material with calcite mesocrystal fibres of cross-sections in the 10 micrometer range and lengths exceeding 200 micrometers, and (3) columnar calcite composed of crystals with cross-sections in the 100 micrometer range and lengths reaching almost 1 mm.

Depósito legal: CA-602-2004 / ISSN: 1698-5478

Length Scale	Feature
molecular	substances: $CaCO_3$, lipids, polysaccharides, proteins
10-1000 nanometers	primary $CaCO_3$ particles, calcite nano-fibrils, organic membranes
1-10 micrometers	fibrous or columnar mesocrystals composed of primary particles
10-100 micrometers	arrays of fibres, sub-layers of shell layers
100-1000 micrometers	valve main layers with different microstructure: (1) nano-to-micro-crystalline primary layer (2) fibrous layer (3) columnar layer
millimeters	skeletal elements
centimeters	macroscopic shape

tabla 1. Overview of the hierarchical structure of calcitic brachiopod shells.

3.2. Detailed Description

3.2.1. Molecular level:

The role of intra-crystalline organics and amorphous precursors

For calcitic brachiopods, about 98 % of the shell is calcite - as identified by classical diffraction methods - albeit with absolutely non-classical mineral morphology. The remainder is organic material. The presence of organic macromolecules within the calcite crystals can be seen in the transmission electron microscope *(Fig. 1)* as contrasts that appear to have some crystallographic orientation *(Schmahl et al., 2008, Griesshaber et al., 2009)*. It is still a matter of debate and research, how the $CaCO_3$ is transported to and deposited at the location where it is finally found in the shell material. Williams (1968) claims to have observed vesicles filled with $CaCO_3$ in the cells of the mantle epithelium. These vesicles would then be exocytosed and attached to the mineral forming the shell. This very plausible observation nevertheless needs corroboration by modern studies.

Under TEM conditions we observed in a modern brachiopod shell a large compartment consisting of amorphous calcium carbonate *(ACC, Fig. 2)* in the typical shape of a micro-scale brachiopod calcite fibre. Under TEM conditions (electron irradiation, UHV) the ACC in this compartment crystallized to form an aggregate of vaterite and calcite crystallites *(Fig. 2, and Griesshaber et al., 2009)*. The ACC compartment was located near a defect of the shell which had been repaired by the animal when it was still alive. This observation suggests that at the onset of brachiopod shell formation the first-formed material is ACC, which then crystallizes into one of the crystalline $CaCO_3$ polymorphs, depending on the organism in question. This scenario explains that organic molecules are occluded in the $CaCO_3$; these are remnants from vesicle walls and/or molecules preventing premature crystallization of the ACC.

Pokroy et al. (2006) have shown for many carbonates of biologic origin, that heating

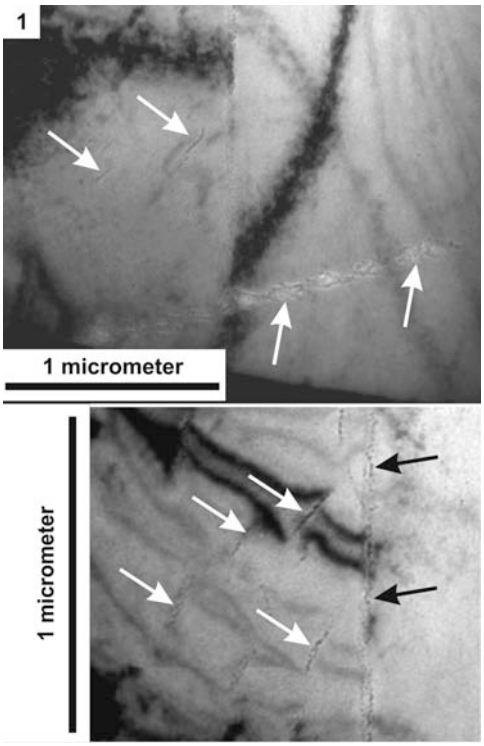

fig. 1. TEM images of a FIB-prepared section of fibrous calcite crystals of the modern brachiopod Megerlia truncata. Even though TEM image contrasts are dominated by bend contours (black stripes within the images) traces of intra-crystalline organic polymers within the biocalcite are well visible and are indicated by white arrows. The black arrows indicate grain boundaries between the micro-scale fibrous crystals. In the grain boundary of the lower image biopolymers are visible. Note that the bend contours are discontinuous at the locations of the organic molecules.

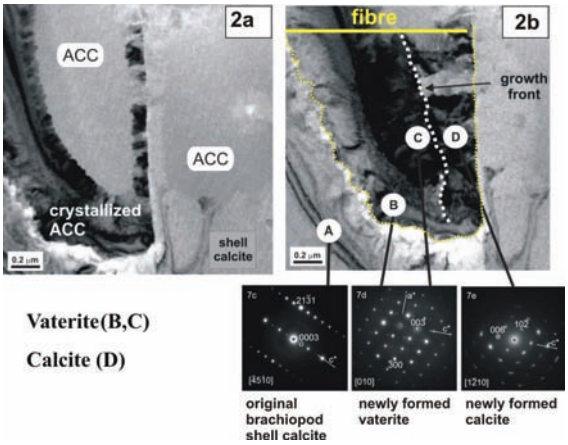

fig. 2. TEM images showing an ACC compartment within a fibrous layer of the brachiopod Megerlia truncata. The compartment has the typical shape of a brachiopod calcite fibre. Under TEM conditions vaterite and calcite crystals crystallize in-situ from the ACC. Fig. 2a shows the ACC compartment shortly after the start of the crystallization, while in Fig. 2b the newly formed crystals have grown together along a seamless growth front (dotted line). Below Fig. 2b diffraction patterns of the original brachiopod shell calcite marked ''A'' and diffraction patterns of the newly formed vaterite crystals, marked ''B'' and ''C'' are given. The diffraction pattern from the newly formed calcite is marked ''D''.

of the material to 200°C results in a relaxation of the lattice parameters of the carbonate mineral, such that it is likely that the intra-crystalline organics strain the lattice, and the strain is released upon the decomposition of the biomolecules on heating. A recent accurate study of *Gaspard et al. (2008)* has shed some light on the molecular constitution of the organic material in the shell, but it remains enigmatic owing to its complexity. Three major types of macromolecules are typically considered as relevant in biominerals: (i) phospholipids, which are the fundamental molecules composing biological cell membranes and vesicle membranes, (ii) polysaccharides, where chitin is the most abundant form used as a structural material by animals *(Al-Sawalmih et al., 2008, Fabritius et al., 2009)*, and (iii) proteins, which are ubiquitous in all tissues, controlling functions (e.g. morphogenesis, Ca- and proton pumping, etc.) as well as strength *(e.g. collagen in bone, Currey, 2006)*. According to *Gaspard et al. (2008) relatively high amounts of glucosamine may suggest the presence of chitin in the shell matrix* of the investigated rhynchonelliform brachiopods, while the group found several

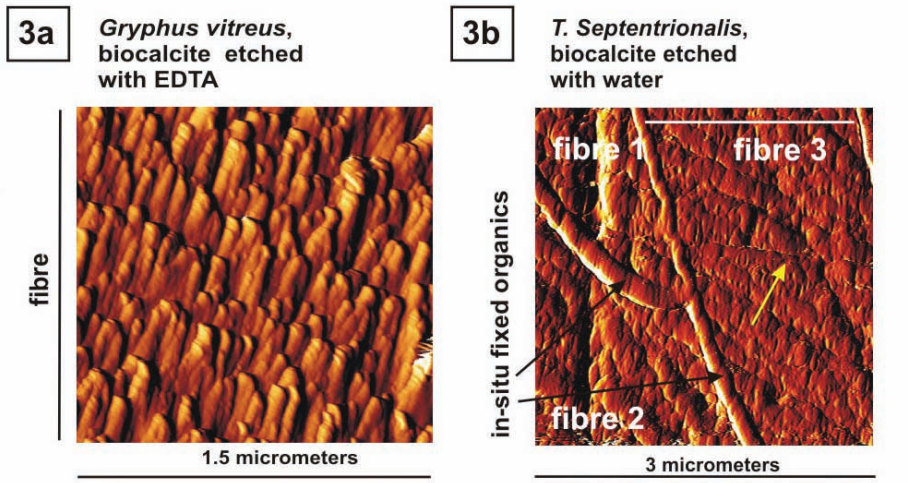

fig. 3. AFM images of the internal nanostructure inside micro-scale calcite fibres from the valves of G. vitreus (a) and T. septentrionalis (b). These structures are visualized through etching the sample either with distilled water or with EDTA solution. Etching dissolves the uppermost calcite layers and leaves behind the organic coating around the micro-scale fibrous crystals and makes the nano-fibrils visible (Fig. 3b) that are present within the fibres. The protruding organic sheaths and membranes emerge from the surface of the sample (Fig. 3b).

Depósito legal: CA-602-2004 / ISSN: 1698-5478

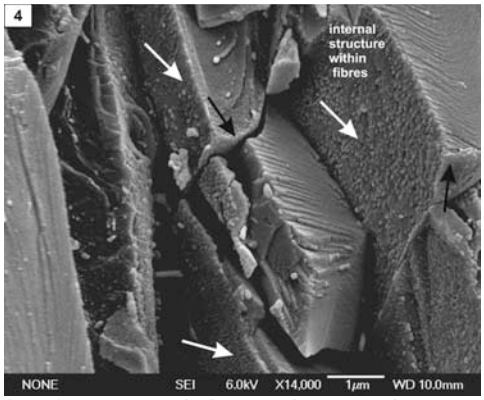

fig. 4. SEM micrograph of a fracture surface sample of the modern brachiopod species Terebratulina septentrionalis. The biopolymers present within the shell were fixed chemically subsequent to the removal of the adult animal from the water. The nano-fibrils composing the micro-scale crystal fibres are visible as protrusions on the flat/concave side of the fibres (white arrows) and on the fracture surface (e.g. top right of image). The black arrows point to the convex sides of the fibres where the organic sheath around the fibres is well visible. We followed the fixation procedure of Fabritius et al. (2005).

different proteins of 20-25 kDa, 37 kDa, and 50 kDa in different species as well as low molecular weight glycoproteins. *Cusack et al. (2000)* had reported a 62kDa glycosylated protein.

3.2.2. Nanostructure-Level

Fibrous Main Layer Material

The comments on organic membranes in the discussion of the molecular level above directly lead to the nanostructure level. Careful etching techniques and observations with AFM and SEM reveal what we address as nano scale primary particles composing the calcite crystals of the micro-scale *(Figs. 3 and 4)*. *Fig. 3* shows two images obtained with AFM with etching in-situ into a polished surface of the fibrous calcite layer of two different brachiopod species. In *Fig. 3a* the etching reveals nano-fibrils in *Gryphus vitreus*, which give a vague impression as themselves being subdivided into nanoparticles. Elongated primary nanoparticles of *Terebratulina septentrionalis* can be seen in *Fig. 3b*. Further, the nanoparticles are arranged in nano-scale lamellae. *Fig. 3b* also clearly reveals the organic membranes surrounding and separating the three micro-scale fibre units covered in the image, which form the units of the next-higher level of structural architecture. The nanofibrils compose micro-scale units which have a crystallographically coherent lattice (see description of the micro-scale levels). For objects which are composed of nano-scale crystallites building an aggregate with a coherent 3D crystallographic lattice the term *mesocrystal* has been coined *(Xu et al., 2007; Gebauer et al., 2008, Meldrum & Cölfen, 2008, Xu et al., 2008)*. The SEM micrograph of a fracture surface *(Fig. 4)* also highlights the mesocrystalline constitution of the calcite microfibres of the brachiopod species *Terebratulina septentrionalis*. The nano-fibrils are revealed both at trans-granular cracks as well as by the lawn of nano-scale protrusions of the nano-fibrils at the interfaces of the mesocrystal fibres. *Fig. 5* displays high-resolution SEM micrographs of the micro-scale mesocrystal fibres as seen both from their curved convex surfa-

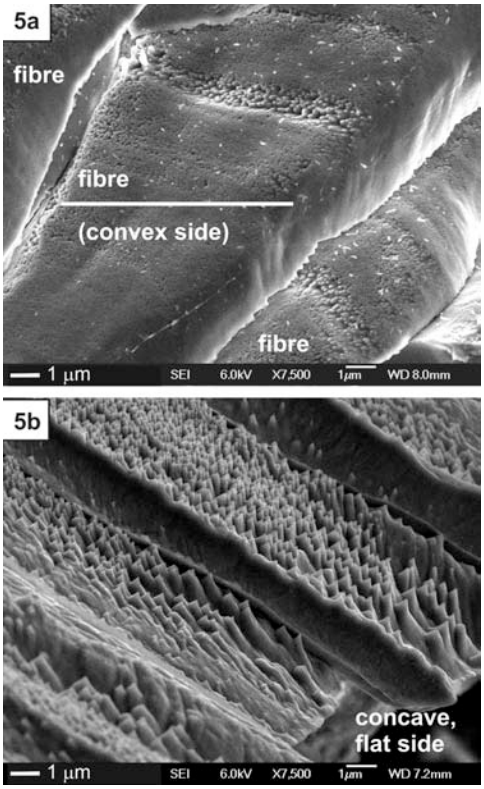

fig. 5. SEM micrographs showing the mesocrystalline constitution of micro-scale calcite crystal fibres of a juvenile specimen of Terebratulina septentrionalis. The organic polymers were fixed chemically. The mesocrystal assemblage of nano-fibrils composing the micro-scale fibrous crystals is well observable both on the curved convex (a) and the flat/concave (b) surfaces of the fibres (refer to Fig. 10 for another view of convex and concave sides of brachiopod calcite fibres).

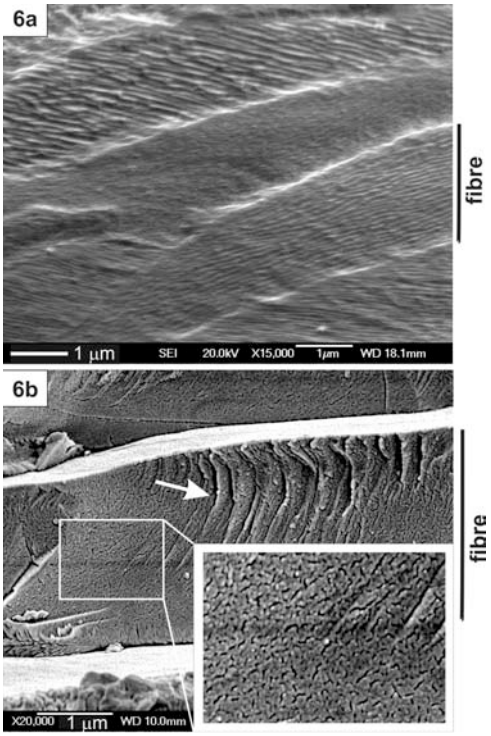

fig. 6. Internal mesostructure of micro-scale calcite crystal fibres of T. septentrionalis. In etch-polished surfaces the internal structure is visible as a lamination (a). The lamellae build arrays and have a coherent orientation within a certain fibre; neighbouring fibres are tilted crystallographically relative to each other. Higher SEM magnification resolves further internal structural details within the fibres (b). Irregularly shaped black voids are visible. These contained the organic polymers within the fibres but are destroyed under SEM conditions at the surface of the imaged sample. The white arrow in Fig. 6b shows the typical conchoidal fracture behaviour of the fibrous biocalcite. The white lining on top of the fibre in Figure 6b highlights the organic sheath that is wrapped around all brachiopod calcite crystal fibres.

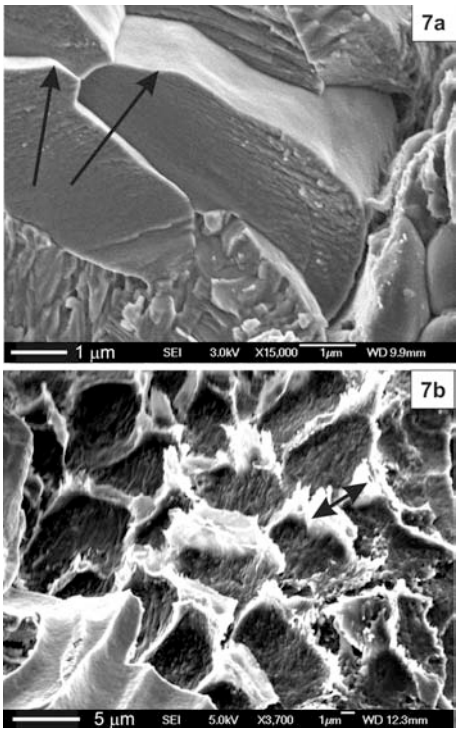

fig. 7. SEM images of fracture surfaces of adult Gryphus vitreus (a) and juvenile Terebratulina septentrionalis (b). Organic sheaths around the fibres (arrows) and the internal lamination within the fibres due to their mesocrystalline nanostructure are visible. For Fig. 7b the shell was treated by chemical fixation of the biopolymers prior to fracturing the sample; the organic coating around the fibres is exceedingly well visible.

ces and their flat/concave surfaces. Zooming out from the nano-fibrils, the layered packing of the nano-fibrils within the micro-scale fibres becomes visible *(Figs. 6a and 6b)*. We attribute the nano-fibril constitution to the existence of the extremely thin organic membrane molecules visible in TEM *(Fig. 1)*, which are not directly visible in our AFM and SEM pictures. Those molecules do not appear to form membranes which completely encapsulate nano-compartments, but they appear to be disrupted, allowing the calcite around them to form a coherent crystal lattice, which terminates at the larger and stronger membranes which can be seen separating the three micro-scale fibres in *Fig. 3b*. In *Fig. 5b* those membranes appear as deeper-etched canals between the calcite fibres. In *Fig. 7* the membranes show in the SEM contrast. If the membranes are fixed *in-situ* chemically they obtain increased tensile strength and stick out of fracture surfaces like tattered cloth *(Fig. 7b)*.

Cusack et al. (2008) showed AFM pictures of *Terebratulina retusa* where triangular nano-scale features could be seen pointing all in a parallel direction. The authors addressed these features as the primary particles. We did not find such triangular structures in our very careful studies. Just like *Cusack et al. (2008)* we used the common triangular pyramidal AFM sensors. We made sure we frequently replaced tips worn out by usage by fresh and unbroken sensor tips.

Primary Main Layer Material

The grain size of the outer primary layer material is on the scale of hundreds of nanome-

Depósito legal: CA-602-2004 / ISSN: 1698-5478

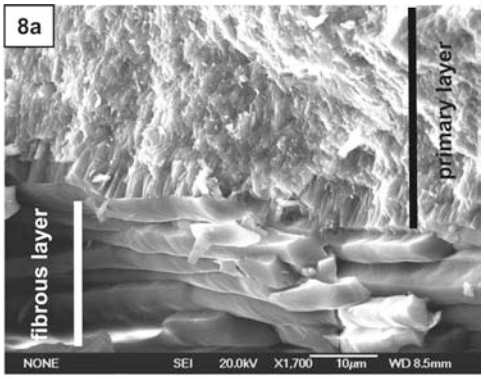

fig. 8. (a) SEM image of a fracture surface sample of the modern brachiopod Megerlia truncata showing the nano- to micro-scale calcite crystal assemblage of the primary layer and the contact to the fibres of the adjacent fibrous layer. The arrow indicates the ordered succession of calcite lamellae at the contact of the primary to the fibrous layer. (b) TEM images from a tilt series highlighting the individual crystallites and their interlocking fabric within the primary layer of Megerlia truncata (FIB prepared sample).

tres *(Fig. 8 and Schmahl et al., 2004, Griesshaber et al., 2007, Goetz et al., 2009, Griesshaber et al. 2010)*. The scale of those grains is similar to that of the primary particles composing the calcite fibres. However, the primary layer nano-grains have an irregular shape and form an interlocked structure *(Fig. 8b)*. With our TEM observations we so far did not see organic components within or around the grains. For the transport of the calcium carbonate in place and for the control of formation of the interlocked nanostructure we assume that biologic membranes at least must have been existing. They may be too thin to be visible in TEM (we were not able to achieve atomic resolution due to beam damage on the calcite). If there are organics in the primary layer they are much less abundant than in the fibrous layers and they are of a different kind.

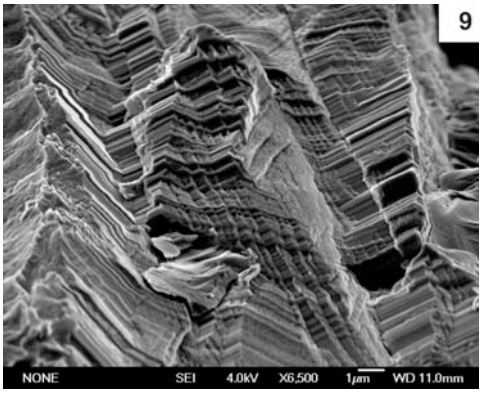

fig. 9. SEM micrograph of calcite crystals the columnar layer of Gryphus vitreus displaying their massive appearance in comparison to fibrous calcite. Well-aligned parallel surface kinks are visible. This feature could be due to an internal structure of parallel lamellae, but their perfect arrangement also suggests a simple inorganic crystallographic origin such as cleavage steps. Columnar layer brachiopod calcite resembles non-biological calcite to a high degree.

The interlocked nano-scale structure of this material leads to a high hardness in micro-scale Vickers indents, reaching values twice as high as single-crystalline geologic calcite *(Griesshaber et al., 2007, Schmahl et al., 2008)*. By comparison, for micro-scale indents larger than the fibre diameter, the hardness of the fibrous layer is equal to or less than that of geologic calcite due to delamination of the fibres at the organic sheath.

fig. 10. Perfect cross section through an array of fibrous calcite crystals of Megerlia truncata and a sketch indicating a typical fibre with its crystallographic orientation. Note the convex and concave sides of the fibres.

Columnar Layer Material

The columnar layer material *(Fig. 9)* is the least well investigated so far. These crystals appear much like inorganic crystals. We see a "lamination" on the sub-micrometer scale in SEM micrographs of fractured samples, but it is impossible to exclude that this feature is due to faceting related to cleavage.

3.2.3. Microstructure level 1: single crystals fibres or columns

Fibrous Main Layer Material

The fundamental unit at the micro scale are the calcite mesocrystal fibres which each have uniform crystallographic orientation (at least within the ± 0.3° resolution of the EBSD technique) throughout their length. The shape of such a fibre is schematically shown in *Fig. 10* together with an SEM micrograph of cross-sections through a typical stack of fibres. The fibres are sheathed by a continuous organic membrane. Depending on the brachiopod species, the fibre length can reach more than 200 micrometres, and their width is typically in the range of 2-20 micrometers. EBSD shows that the crystallographic c-axis (triad axis) of the calcite is perpendicular to the morphological axis of the fibre *(Fig. 11,* and *Schmahl et al., 2004, Griesshaber et al., 2007, Griesshaber et al., 2010)*, while the morphological axis of the fibre can be in any direction in (or nearly in) the crystallographic a-b plane *(Fig. 10)*. The morphological axis varies both within a given fibre as it is curved (while the crystallographic lattice remains constant), and it usually varies from one fibre to the next in a fibre pack.

Columnar and Primary Main Layer Material

The two materials with less involvement of organic material show less unusual features. The large and apparently simple calcite columns *(Fig. 9, Fig. 11c, Fig. 12)* have their calcite c-axis parallel to the axis of the column, while the column is perpendicular to the shell surface. It can be seen that a single column can abruptly branch-off a single fibre at the contact of the columnar and the fibrous layer: here the crystallographic lattice orientation remains the same while the long axis of the morphological shape describes more or less a right angle at the branch *(Fig. 12b, columns marked in red, and Fig. 13b)*.

In the primary main layer micro-sized crystals are frequently found in a layer adjacent to the fibrous layer. Research on their nature is pending, but what can be said at this stage is that they show aspects like a miniature expression of the columnar calcite (see the lengthy crystals of the primary layer in *Fig. 8a* and *Fig. 11a* with c-axis parallel to their length).

3.2.4. Microstructure level 2 - Fibre Packing and fibre sub-layers, column packing

Fibrous Main Layer Material

The EBSD technique (Griesshaber et al., 2010) adequately reveals the micro-scale structure of the different calcite-based materials used by brachiopods to build their shell valves and their hinge (an investigation of the brachidium is still pending). In the sub-layers of the fibrous layer (called the secondary layer for two-layered brachiopods and tertiary layer for three-layered brachiopods) the micro-scale mesocrystal fibres are stacked in parallel to form an interlocking microstructure as displayed in *Fig. 10. Fig. 11a* and b show EBSD maps of the crystal orientation in such packings. These maps cover areas, where sub-layers can be seen containing fibres sectioned in different orientation, longitudinal and transversal. In this way a plywood-like structure is formed on the scale of tens of micrometers. Plywood-like structures are a common measure to improve material strength and toughness in hierarchical fibre composites. They are found in vertebrate bone *(Weiner et al., 1999)*, lingulid brachiopods *(Schmahl et al., 2008, Merkel et al., 2009)*, and in the cross-laminated layer of molluscs *(Kamat et al., 2000)*.

Columnar and Primary Main Layer Materials

Fig. 11c shows the microstructure of the columnar layer of *Gryphus vitreus* and *Fig. 12* shows EBSD maps of another prominent example displaying a columnar layer,

Depósito legal: CA-602-2004 / ISSN: 1698-5478

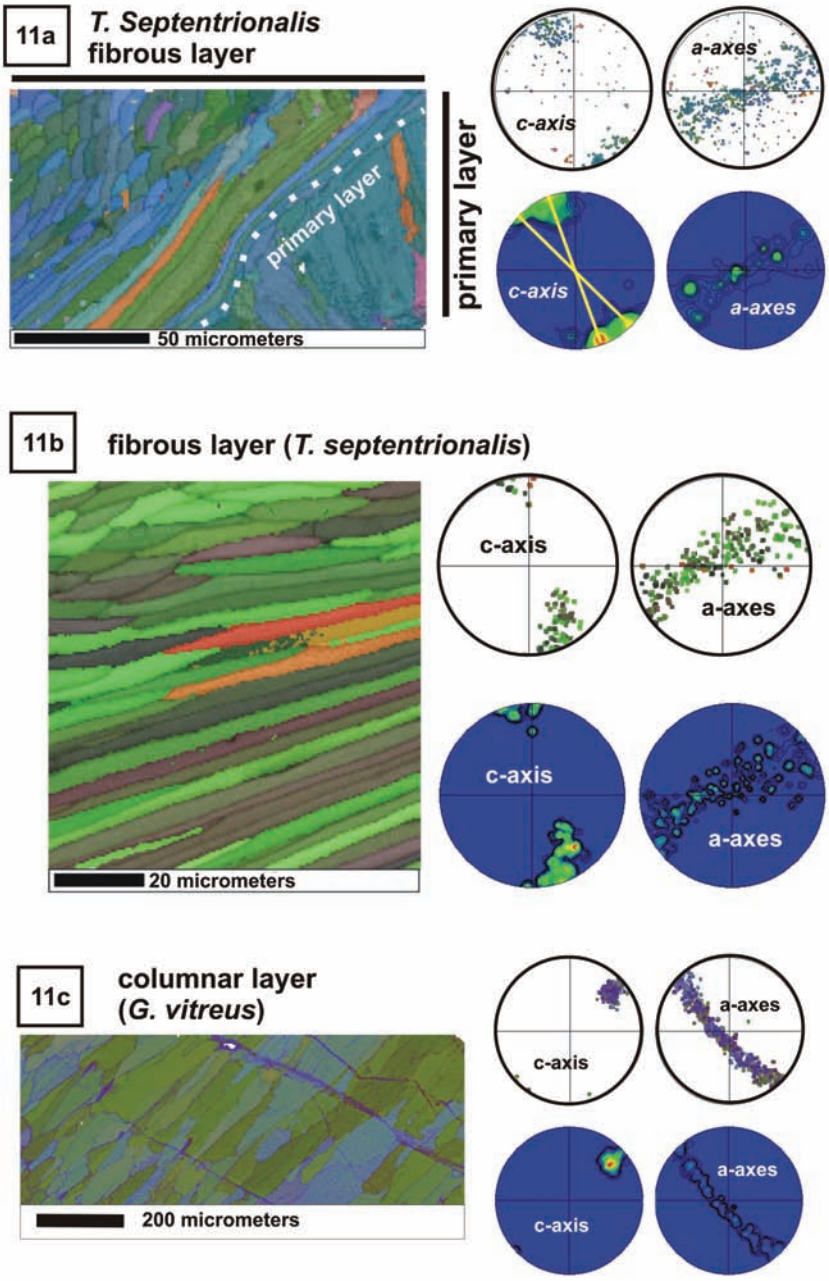

fig. 11. EBSD maps of crystallographic preferred orientation (texture) of biological calcite forming the different shell layers of the modern brachiopods Terebratulina septentrionalis (Figs. 11a, 11b) and Gryphus vitreus (Fig. 11c). Colour coding of the maps represents the three orientational angles of the crystal lattice as RGB colours. Note that uniform colours in an area of a map indicates uniform orientation of the crystal lattice in this area. The adjacent pole figures show the stereographic projections of the crystal axes in the colours corresponding to the map and as a pole density plot, respectively. While Figs. 11a and 11b highlight the texture of the primary and the fibrous shell materials (fibres cut in both directions, perpendicular and transverse), Fig. 11c shows the crystallographic preferred orientation of the columnar material. Note that for the fibrous calcite the c-axis is perpendicular to sub-perpendicular to the fibre while for the columnar layer the c-axis is parallel to the column.

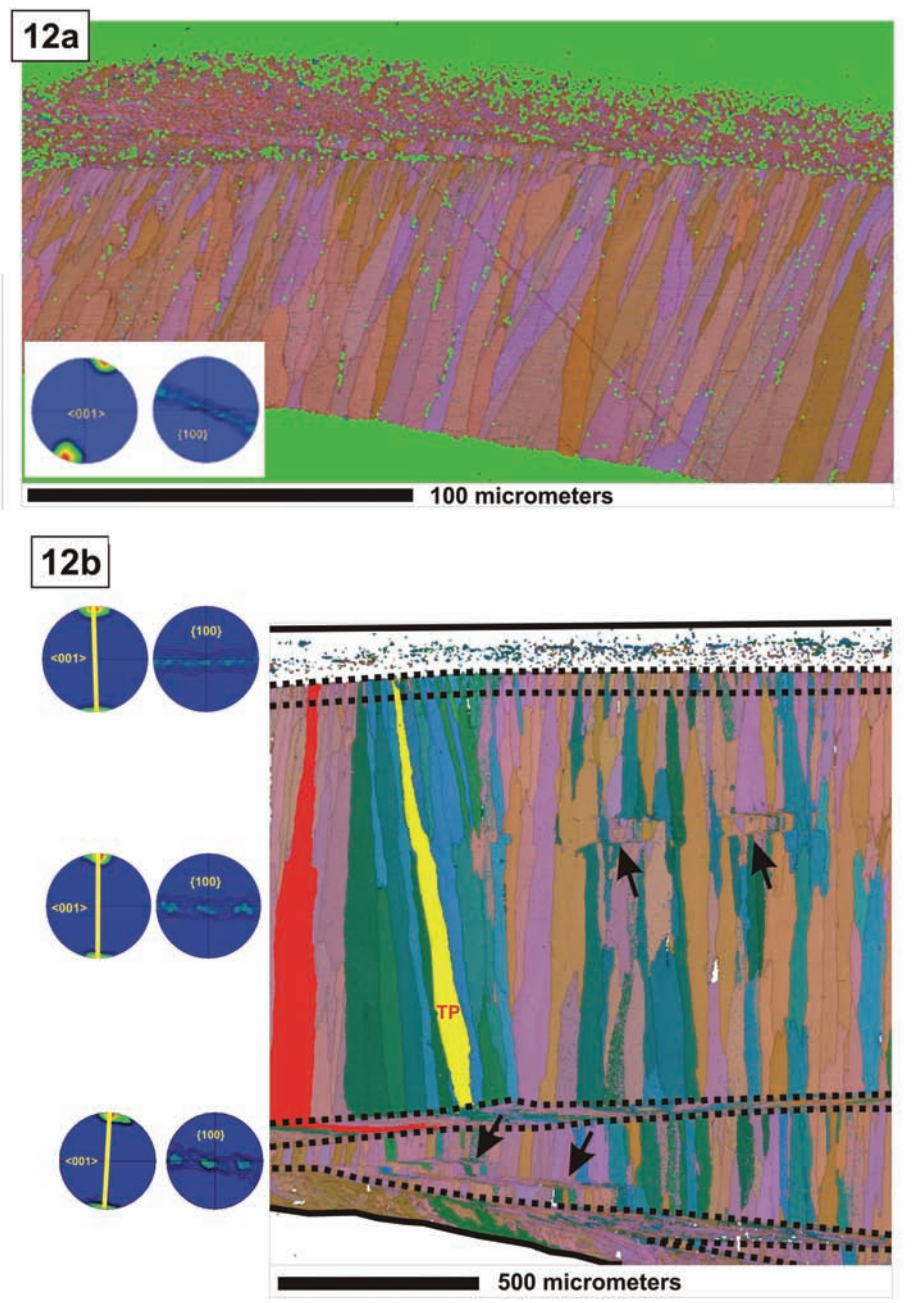

fig. 12. EBSD maps of the primary and the columnar layers of Liothyrella neozelanica. Note the large columnar units within this shell layer and the identical, well defined, sharp cylindrical textures of the columnar layer and the primary layer. EBSD map colouring is given in RGB colour coding of the Euler angles. Note the branching-off of fibres from the columns at the bottom end of the columnar layer in (b) and the successive coarsening of the columnar crystals as they nucleate at the primary layer and competitively grow away from it with the c-axis as the fastest axis of growth (Goetz et al., 2009).

Liothyrella neozelanica (Goetz et al., 2009). The columnar structure shows a pattern of increasing column width from the contact zone at the primary layer towards the inside of the shell *(Fig. 12)*. The crystallographic preferred orientation of this layer is very sharp *(Fig.12)*. Both texture and columnar arrangement suggests that the columns form by a competitive growth mechanism starting at the contact to the primary layer. This mode of growth and texture formation has been described for the calcite of the avian egg shell *(Rodríguez-Navarro & García-Ruiz, 2000; Dalbeck & Cusack, 2006)*.

The primary layer is differentiated into sub-layers, as can be seen by careful inspection of *Figs. 8a, 12a, and 13a*. Usually nano-scale material is on the outside, while micrometer-sized columnar or platelet-shaped crystals form a sub-layer which is in contact with the fibrous layer which follows to the inward of the valve *(e.g. Schmahl et al. 2008; Goetz et al. 2009, Griesshaber et al. 2010)*. As already pointed out in the discussion of microstructural level 1 above, these coarser crystals look like a miniature form of the columnar calcite, and this ties in with the observation that the nucleation stage of the competitive growth of the crystals building the columnar layer originates at the primary layer *(Fig.12)*.

3.2.5. The main layering with up to three distinct calcite microstructures

The valves of modern brachiopod shells are usually composed of two or three distinct layers of the different material microstructures described above: fine-scaled primary layer, columnar layer, fibrous layer. In addition, the outside of the shell is covered by a thin organic membrane, the periostracum. Depending on the species, the primary layer is usually 50-100 micrometers thick , the fibrous layer can reach some hundreds of micrometres in thickness, and the columnar layer can reach one millimetre. For all calcitic brachiopods the outermost (primary) layer of the valve is formed by the fine grained, nano-to-micro-scale primary layer material *(Fig. 12, Fig. 13a)*. The succession of three layers - primary - fibrous - columnar for *Gryphus vitreus* is depicted in *Fig. 14*. For *L. neozelanica* the columnar layer always follows inward below the primary layer. The fibrous layer is not present at the commissure and it increases in thickness towards the umbo, where it is much thicker than the columnar layer *(Goetz et al., 2009)*. *L. neozelanica* nevertheless shows occasional interlayering of fibrous material into columnar material *(Fig. 12)*. For *G. vitreus* the arrangement of fibrous and columnar material is quite irregular.

3.2.6. Macroscopic morphology: skeletal elements and macroscopic shape

Macroscopically, the shells consist of two valves connected at the hinge. *Fig. 16* shows photographs of the shells of two brachiopod species. Unlike bivalve molluscs, each of the brachiopod valves has a mirror plane (median plane) and the two valves are not connected by a left-right symmetry. The animals grow continuously and they continuously mineralize calcite mainly, but not exclusively, at the margin of the shell, the commissure, which always forms the youngest part of the shell. The mineralization is driven by the epithelial cells of the mantle tissue. The oldest part of the valves is the primary layer at the outer rim near the hinge *(Fig. 15, Fig. 16 and Griesshaber et al., 2010)*. The mineralization process at the comissural margin leads to a logarithmic spiral equation for the development of the shape as demonstrated by *Rudwick (1959)*. Forming at the oldest part of the shell is the umbo. This shell region contains an opening for the muscular pedicle by which the animal attaches to the substrate. The macroscopic morphology of the brachiopoda is quite diverse and very interesting in itself, but we refer to the palaeontological literature for details *(Rudwick, 1970, Williams et al., 2000)*.

The valves have quite constant thickness. As described in *Griesshaber et al. (2010)*, juvenile individuals show thinner valves than older individuals, and, accordingly, growth of the valve does not occur exclusively at the commissure - mineralization is needed to increase the thickness in the posterior parts of the shell. From our observations on *L. neozelanica* we learn from the lack of the fibrous layer at the commissure and its increase

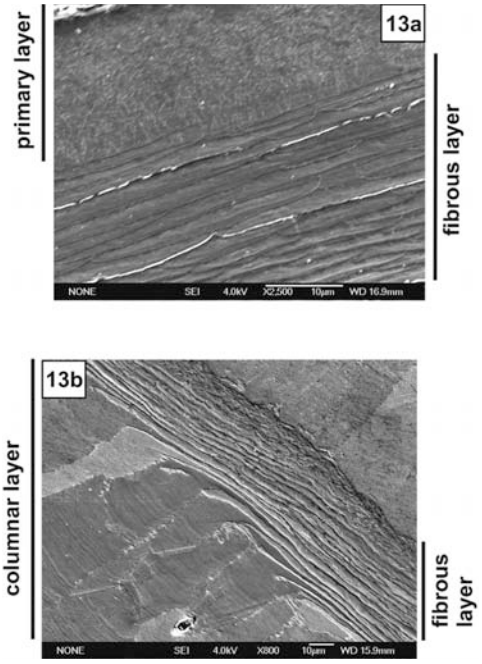

fig. 13. SEM orientation contrast images of the primary and the fibrous shell layers of T. septentrionalis (a) and the columnar layer of G. vitreus (b) where a stack of fibres branches off from the columns.

towards the umbo, that this fibrous material is added by the epithelium at the inside of the valve. The umbo and hinge region needs permanent strengthening and reconstruction owing to a complex shape of interlocking protrusions from both valves at the hinge.
The calcite of the brachiopod shells shows a pronounced pattern of crystallographic preferred orientation *(Schmahl et al., 2004, Griesshaber et al., 2007, Griesshaber et al., 2010)*, which connects the molecular scale structure with the architecture on the macroscopic scale: The crystallographic c-axes (triad axis) of the calcite crystal structure shows a sharp maximum of the orientational probability density in the orientation perpendicular (or sub-perpendicular) to the shell vault *(Schmahl et al., 2004, Griesshaber et al., 2007, Fig. 15)*.

4. Discussion

4.1. What is the gain of the hierarchical structure?

With its hierarchical composite structure the

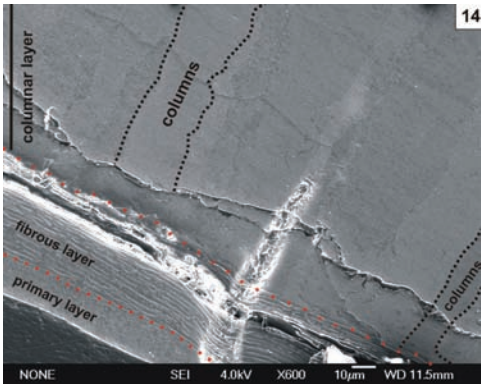

fig. 14. Overview of the three shell layers of Gryphus vitreus. The outer, nanocrystalline primary layer is followed inward by the fibrous layer. The innermost shell layer along almost the entire length of the valve (except for the commissure) consists of the columnar layer.

biocalcite is very distinct from inorganic calcite. They have only the gross chemical composition $CaCO_3$ and the molecular level (crystal) structure in common. The structuring or architecture of the biocalcite is controlled by organic membranes, which compartmentalize space and thus control morphogenesis on all length scales. While the chemical components of calcite are abundant and readily available to marine organisms, calcite is also extremely brittle and useless as a structural material, unless it is moulded into a composite material with improved mechanical performance. It appears that amorphous calcium carbonate is used to fill the compartments created by the organic matrix, as the amorphous material has no own demands on shape, and it is turned into calcite *in situ (Griesshaber et al., 2009)*. In this way matrix molecules are incorporated and a mesocrystal is the result. *Fig. 17* shows an EBSD map of a calcite mesocrystal grown in a methacrylate gel. Here the compartmentalization is given by the gel pores; crystal growth must proceed from pore to pore, loosing gradually crystallographic coherence in the process.

Apart from the morphogenetical role the biologic macromolecules turn the extremely brittle calcite into a useful structural material. The organics alone are disadvantageous for a shell structure. In the composite, the mineral provides a high elastic modulus *(i.e. stiffness)* to the skeleton, such that an effective loading frame for the amplification of muscle action is provided. The mineral further provides compressive strength,

Depósito legal: CA-602-2004 / ISSN: 1698-5478

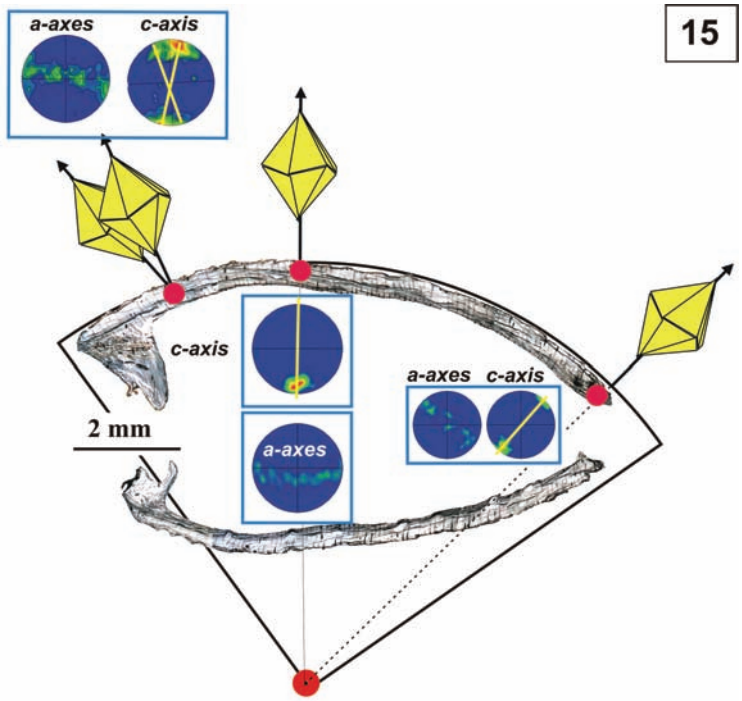

fig. 15. Cross section along the median plane (mirror plane) of the valves of Megerlia truncata together with pole figures for the calcite a- and c-axes measured by EBSD at the indicated points. Brachiopod shell calcite c-axes usually are found perpendicular to the vault - parallel to the radius of curvature - of the shell (Schmahl et al. 2004, see Griesshaber et al., 2007 for more pole figures corroborating the result). A sharp uniaxial fibre texture is present within both valves. However, in the older parts of the shell near the hinge a bi- or multi-modal distribution pattern of c-axes is observable (Griesshaber et al. 2007), even though the shell microstructure of the hinge is similar to that of the valves.

bending strength, hardness, and abrasion resistance to the shell. The organic component of the composite provides tensile strength, flexibility, and, to a certain degree, ductility. However, the composite is more than the sum of its parts. Our micro- and nanoindentation measurements *(Griesshaber et al., 2007; Schmahl et al., 2008; Merkel et al., 2009)* provide a measure of

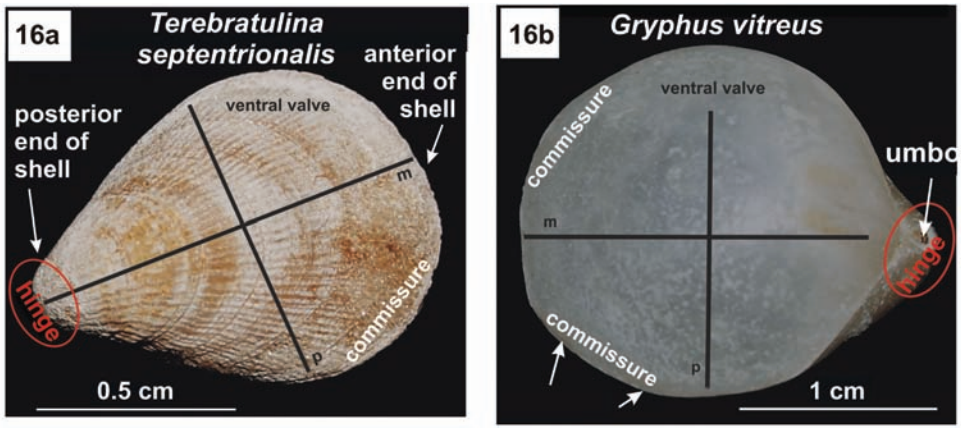

fig. 16. Images of the ventral valves of the modern brachiopods Terebratulina septentrionalis (a) and Gryphus vitreus (b). While T. septentrionalis has a two-layered shell structure composed of the primary and the fibrous layers G. vitreus builds a three layered shell that consists of the primary, the fibrous and the columnar shell layers. Black lines in both figures indicate the orientations of the wafers that were cut out for from the shells for preparation of thin sections.

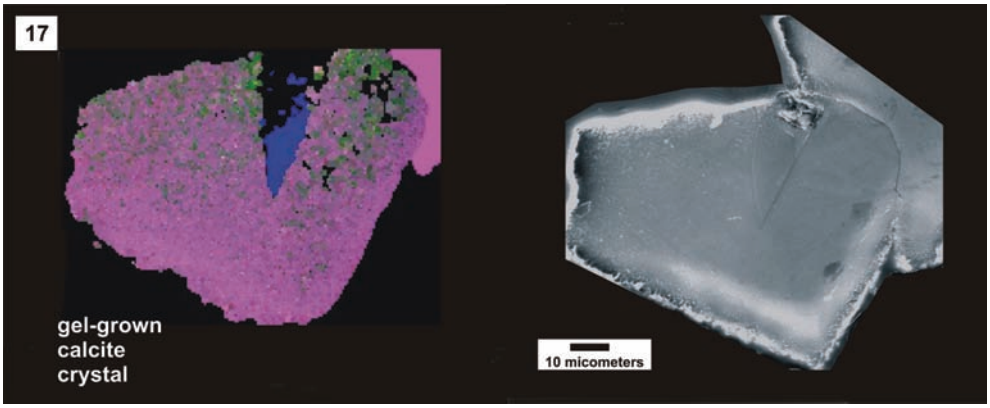

fig. 17. Image of a gel-grown synthetic calcite crystal. The upper image shows a colour-coded EBSD map of the crystal, while the lower image gives the corresponding SEM micrograph. The EBSD map highlights well the mesocrystalline microstructure of the gel-grown calcite crystal.

strength of the composite material. The presence of the biomolecules inside the fibrous calcite crystals increases the hardness probed by a nano-scale indent by a factor of two compared to inorganic calcite. Essentially, the intra-crystalline organics impede the motion of dislocations and they thus also prevent the (104) cleavage of the calcite. The organics *between* the calcite fibres form a flexible adhesive between the fibres. It makes the material softer to micro-scale indents as it allows the fibrous microstructure to tolerate a certain degree of deformation by dislodging of the fibres without the brittle failure which would occur in pure calcite. The fibre composite microstructure diverts and breaks up cracks into many subcracks, which run mainly parallel to the fibres and parallel to the shell surface rather than perpendicular to it. In this way the energy of the crack is consumed and the fracture toughness of the material is increased.

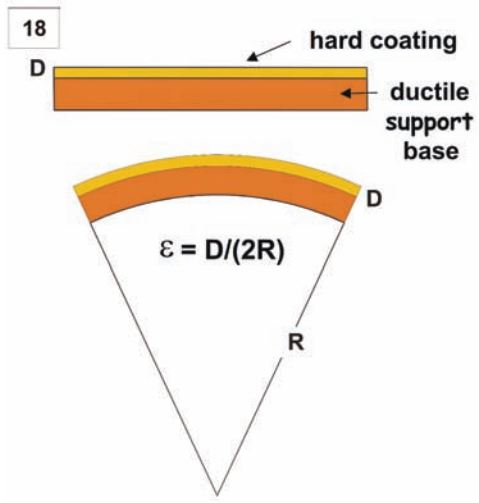

fig. 18. Bending strains in a material are proportional to thickness. A hard protective outer layer covering a compliant base material must be kept thin to allow compliant bending of the structure with minimal risk of brittle fracture of the cover layer. This design principle is observed in many biologic structures.

The composite material architecture also allows for adaptation of the material properties using the same basic recipe for the material. This is used in the main shell layering. A brittle shell would hardly be an evolutionary advantage unless strength is achieved by thickness (as in the shells with columnar layers). A tough hybrid (organic/inorganic) fibre-composite shell material, with its substantial and biologically expensive organic component, on the other hand, is prone to attack by bacteria or by the enzymes of predators. It can be protected by a suitable coating. For the outer, primary calcite layer there are no large inter-crystalline organic membranes. The interlocking nano-scale grain fabric provides a high hardness and stiffness but this also makes the material brittle *(Griesshaber at al., 2007, Schmahl et al., 2008)*. The layered structure of the calcitic brachiopod thus offers an advantage: The resistive, hard protective cap is constructed as a very thin layer on the outside of the more ductile and tough fibre-composite material forming the main body of the thin shell of two-layered brachiopods. If the whole body bends under an applied load, a thin layer is less likely to break or chip-off than a thicker layer, as the bending stresses in a solid layer

are proportional to thickness *(Fig. 18)*. This principle is used for the shell of the phosphatic brachiopod *Lingula anatina (Merkel et al., 2009)*, where thin mineralized layers alternate in a laminate with purely organic layers. The design principle of a hard thin cap on a more ductile base is used e.g. in our teeth (hard enamel on dentine, *Currey, 1996*) and in protective armour technology.

Acknowledgements

We are indebted to E. Kessler, T. Westphal, D. Dettmer and R. Enders for the skilful preparation of samples and we would like to thank A. Bitner, Warszawa, for the *Gryphus vitreus* specimens and A. Ziegler, Ulm, for continuous advice. The help of Lurdes Fernández-Díaz by editing the manuscript and financial support by the German Research Council (DFG) is gratefully acknowledged.

References

Al-Sawalmih, A., Li,C., Siegel, S., Fabritius, H., Yi, S., Raabe, D., Fratzl, P. & Paris, O. (2008) Microtexture and chitin/calcite orientation relationship in the mineralized exoskeleton of the american lobster. Adv. Funct. Mater., 18, 3307–3314

Auclair, A.C., Joachimski, M. M. & Lecuyer, C. (2003) Deciphering kinetic, metabolic and environmental controls on stable isotope fractionations between seawater and the shell of Terebratalia transversa (Brachiopoda). Chem. Geol., 202, 59-78.

Barthelat, F. & Espinosa, H.D. (2007) An experimental investigation of deformation and fracture of nacre–mother of pearl. Exp. Mech., 47, 311–324.

Brand, U., Logan, A., Hiller, N. & Richardson, J. (2003) Geochemistry of modern brachiopods: applications and implications for oceanography and paleoceanography, Chem. Geol., 198, 305-334.

Buening, N. (2001) Brachiopod shells: Recorders of the present and keys to the past, in "Brachiopods ancient and modern; A tribute to G. Arthur Cooper", S. J. Carlson and M.R. Sandy, eds., Pal. Soc. Pap., 7, 117-145.

Carpenter, S. J. & Lohmann, K.C. (1992) Sr/Mg ratios of modern marine calcite: empirical indicators of ocean chemistry and precipitation rate. Geochim. Cosmochim. Acta, 56, 1837- 1849.

_ & _ (1995) $\delta^{18}O$ and $\delta^{13}C$ values of modern brachiopod shells. Geochim. Cosmochim. Acta, 59, 3749-3764.

Currey, J.D. & Taylor, J.D. (1974) The mechanical behaviour of some molluscan hard tissues. J. Zool. (London), 173, 395–406.

__ (1977) Mechanical properties of mother of pearl in tension. P. Roy. Soc. Lond. B Bio., 196, 443–463.

__ (1999) The design of mineralised hard tissues for their mechanical functions. J. Struct. Biol., 202, 3285–3294

__ (2006) Bones: Structure and Mechanics. Princeton Univ. Press, Princeton, New Jersey, 456 pp.

Cusack, M., Laing, J.H., Brown, K. & Walton, D. (2000). Amino acids and proteins of calcitic brachiopod shells. Trends in Comparative Biochemistry and Physiology, 6, 47–56.

__, Dauphin, Y., Chung, P., Pérez-Huerta, A. & Cuif, J.-P. (2008) Multiscale structure of calcite fibres of the shell of the brachiopod Terebratulina retusa. J. Struct. Biol., 164, 96-100.

Dalbeck, P. & Cusack, M. (2006) Crystallography (Electron Backscatter Diffraction) and Chemistry (Electron Probe Microanalysis) of the Avian Eggshell. Crys. Growth Des., 6, 2558-2562.

Fabritius, H., Sachs, C., Romano, P. & Raabe, D. (2009) Influence of structural principles on the mechanics of a biological fiber-based composite material with hierarchical organization: the exoskeleton of the lobster Homarus americanus. Adv. Mater., 21, 391-400.

__, Walther, P. & Ziegler, A. (2005) Architecture of the organic matrix in the sternal CaCO3 deposits of porcellio scaber (Crustacea. Isopoda). J. Struct. Biol., 150, 190-199.

Fratzl, P. & Weinkamer, R. (2007) Nature's hierar-

chical materials. Prog. Mater. Sci., 52, 1263-1334.

Gaspard, D., Marin, F., Guichard, N., Morel, S., Alcaraz, G. & Luquet, G. (2008) Shell matrices of recent rhynchonelliform brachiopods: microstructures and glycosylation studies. Earth Env. Sci. T. R. So., 98, 415-424.

Gao, H.J. (2006) Application of fracture mechanics concepts to hierarchical biomechanics of bone and bone-like materials. Int. J. Fracture, 138, 101–137.

Gebauer, D., Völkel, A. & Cölfen, H. (2008) Stable Prenucleation Calcium Carbonate Clusters. Science, 322, 1819-1822.

Goetz, A., Griesshaber, E., Schmahl, W. W., Neuser, R. D., Lüter, C., Harper, E. M. & Hühner, M. (2009) The texture and hardness distribution pattern in Recent brachiopods – a comparative study of Kakanuiella chathamensis, Liothyrella uva and Liothyrella neozelanica. Eur. J. Mineral. 21, 303–315.

Griesshaber, E., Schmahl, W. W. , Neuser, R. D., Pettke, Th., Blüm, M., Mutterlose, J. & Brand, U. (2007) Crystallographic texture and microstructure of terebratulide brachiopod shell calcite: An optimized materials design with hierarchical architecture. Am. Mineral., 92, 722-734.

__, Kelm, K. Sehrbrock, A., Schmahl, W.W., Mader, W., Mutterlose, J. & Brand, U. (2009) Amorphous components in the shell material of the brachiopod Megerlia truncata, Eur. J. Mineral., 21, 715-723.

__, Neuser, R. & Schmahl, W.W. (2010) The application of EBSD analysis to biomaterials: microstructural and crystallographic texture variations in marine carbonate shells. Seminarios de la Sociedad Española de Mineralogia, 7, 20-30.

Jackson, A. P., Vincent, J. F. V. & Turner R.M. (1988) The mechanical design of nacre. P. Roy. Soc. Lond. B Bio., 234, 415–440.

Kamat, S., Su, X., Ballarini, R. & Heuer, A. (2000) Structural basis for the fracture toughness of the shell of the conch Strombus gigas. Nature, 405, 1036–1040.

Katti, K., Katti, D.R., Tang, J., Pradhan, S. & Sarikaya, M. (2005) Modelling mechanical responses in a laminated biocomposite. Part II. Nonlinear responses and nuances of nanostructure. J. Mater. Sci., 40, 1749–1755.

Lowenstam, H.A. (1961) Mineralogy, $^{18}O/^{16}O$ ratios, and strontium and magnesium contents of recent and fossil brachiopods and their bearing on the history of oceans. J. Geol., 69, 241-260.

Meldrum, F. C. & Cölfen, H. (2008) Controlling Mineral Morphologies and Structures in Biological and Synthetic Systems. Chem. Rev., 108, 4332-4432.

Merkel, C., Deuschle, J., Griesshaber, E., Enders, S., Steinhauser, E., Hochleitner, R., Brand, U. & Schmahl, W.W. (2009) Mechanical properties of modern calcitic- (Megerlia truncata) and phosphatic-shelled brachiopods (Discradisca stella and Lingula anatina) determined by nanoindentation. J. Struct. Biol., 168, 396–408

Mucci, A. & Morse, J.W. (1983) The incorporation of Mg^{2+} and Sr^{2+} into calcite overgrowths: influences of growth rate and solution composition. Geochim. Cosmochim. Acta, 47, 217-233.

Okumura, K. & de Gennes, P.G. (2001) Why is nacre strong? Elastic theory and fracture mechanics for biocomposites with stratified structures. Eur. Phy. J. E, 4, 121–127.

Parkinson, D., Curry, G. B., Cusack, M. & Fallick, A. E. (2005) Shell structure, patterns and trends of oxygen and carbon stable isotopes in modern brachiopod shells. Chem. Geol., 219, 193-235.

Pokroy, B., Fitch, A.N., Marin, F., Kapon, M., Adir, N. & Zolotoyabko, E.S.O. (2006) Anisotropic lattice distortions in biogenic calcite induced by intracrystalline organic molecules. J. Struct. Biol., 155, 96-103

Rodríguez-Navarro, A. & García-Ruiz, J.M. (2000) Model of textural development of layered crystal aggregates. Eur. J. Miner., 12, 609–614.

Rudwick, M. J. S. (1959) The growth and form of brachiopod shells. Geol. Mag., 96, 1 – 24.

__ (1970) Living and Fossil Brachiopods, 199 p. Hutchinson & Co. LTD, London

Depósito legal: CA-602-2004 / ISSN: 1698-5478

Sarikaya, M. & Aksay, I.A. (eds, 1995) Biomimetics, design and processing of materials. Woodbury, New York.

Schmahl, W. W., Griesshaber, E., Neuser, R. D., Lenze, A., Job, R. & Brand, U. (2004) The microstructure of the fibrous layer of terebratulide brachiopod shell calcite. Eur. J. Miner., 16, 693-697.

__, __, __, Merkel, C., Deuschle, J., Götz, A., Kelm, K., Mader, W. & Sehrbrock, A. (2008) Crystal morphology and hybrid fibre composite architecture of phosphatic and calcitic brachiopod shell materials - an overview. Mineral. Mag., 72, 541–562.

Veizer, J., Ala, D. & Azmy, K. (1999) $^{87}Sr/^{86}Sr$, $\delta^{13}C$ and $\delta^{18}O$ evolution of Phanerozoic seawater, Chem. Geol., 161, 59-88.

Weiner, S., Traub, W. & Wagner, H.D. (1999) Lamellar bone: Structure-function relations. J. Struct. Biol., 126, 241-255

__ & Dove, P. M. (2003) An overview of biomineralization processes and the problem of vital effect. Rev. Mineral. Geochem., 54, 1-31.

Williams, A. (1968) Evolution of the shell structure of articulate brachiopods. Spec. Pap. Pal., 2, 1-55.

Williams, A., Carlson, S.J. & Brunton, C.H.C (2000) Brachiopod classification, in Williams, A. et al. Brachiopoda (revised), Treatise on Invertebrate Paleontology (Kaesler, R.L., ed.). Boulder, Colorado: Geological Society of America and Lawrence, Kansas: The University of Kansas, ISBN 0-8137-3108-9.

Xu, A.-W., Ma, Y. & Cölfen, H. (2007) Biomimetic mineralization. J. Mater. Chem., 17, 415-449.

__, Antonietti, M., Yu, S.-H. & Cölfen, H. (2008) Polymer-mediated mineralization and self-similar mesoscale-organized calcium carbonate with unusual superstructures. Adv. Mater., 20, 1333-1338.